

Regularized shape from focus

Rajiv R. Sahay and A. N. Rajagopalan

Image Processing and Computer Vision Lab

Department of Electrical Engineering, IIT Madras, Chennai

sahayitm@gmail.com, raju@ee.iitm.ac.in

Abstract—Shape from focus (SFF) estimates the structure of a 3D object using the degree of focus as a cue in a sequence of observations. The estimate of the depth profile is however, vulnerable to lack of sufficient scene texture. In this paper, we propose a method to improve the estimate of the structure of the object by exploiting neighbourhood dependencies. A degradation model is used to describe the formation of space-variantly blurred observations in SFF. The shape of the object is modeled as a Markov random field and a suitably derived objective function is minimized to arrive at the final estimate of the shape.

Index Terms—Shape from focus, depth recovery, space-variant blur, Markov random fields.

I. INTRODUCTION

One of the techniques used to estimate the structure of a 3D object is shape from focus [1]. It uses the degree of focus in an image as a cue to extract shape. Several attempts have been made in the past to improve upon the depth estimates computed using focus as a cue. Subbarao et. al. fit a low-order polynomial to a few data points lying on the largest mode [2]. In [3], a piece-wise curved local window is proposed for computing the focus measure. Multilayer feed-forward neural networks are used in [4] for finding the shape. A dynamic programming based optimization approach has been proposed in [5] which estimates the shape using the notion of a focused image surface (FIS). The authors in [6] recover shape by maximizing the focus measure in the 3D image volume. In [7] super-resolution of the focused image of the underlying 3D object in SFF is demonstrated. In a recent work, the shape estimate was obtained using relative defocus blur derived from actual image data [8].

The traditional SFF method [1], uses the sum-modified Laplacian (SML) focus measure operator to measure the degree of focus of a pixel in a space-variantly blurred image. The behaviour of the focus measure profile is dependent on the local scene texture. If the texture is weak, e.g. at smooth regions, the estimate of the depth computed by SFF may be far from the true value. The choice of the finite step size for the vertical movement of the translating stage is empirical. Since the shape of focus measure profile depends upon the value of the step size, interpolation may yield erroneous estimates of depth [8]. Also, interpolation is not an ideal way for filling up missing data. If the computation of the depth is made to depend on image data directly, we believe that a better estimate can be obtained.

The depth of a real-world 3D object is generally locally smooth. Traditional SFF however, computes the depth estimate

of every point independent of the depth of the neighbouring points. The focus measure profiles of two adjacent points on the object may result in very different depth estimates. But such a random variation in depth rarely occurs in natural 3D objects.

In this work, we attempt to improve the estimate of the depth map obtained through the traditional SFF method by addressing the above mentioned issues. Since, in SFF, a real aperture camera captures the stack of observations, we describe the process of formation of the sequence of space-variantly blurred images captured in a SFF scenario by a degradation model. We use certain novel features of the mechanism of the process of blurring in SFF to relate the blur induced in different observations chosen from the stack. To account for the local smoothness of the depth of the 3D object, its shape is modeled as a Markov random field (MRF). The proposed algorithm also takes care of the fact that when the depth estimate of a point on the 3D object is correct, the SML operator would return the peak value for the focus measure. An objective function is proposed to estimate the shape profile of the 3D object using space-variantly blurred images taken from the stack in SFF. The cost function is minimized by the iterated conditional modes (ICM) [9] technique. Experimental results show that our algorithm is robust to lack of scene texture and returns an estimate which is significantly superior to the depth map obtained using traditional SFF.

II. SHAPE FROM FOCUS

The traditional shape from focus scheme [1] is depicted in Fig. 1. A 3D object is placed on a translational stage which moves in vertical direction in finite steps of size Δd . The initial position of the stage is denoted by the reference plane. The optics of the camera defines a ‘focused plane’ wherein all the points will be perfectly focused on the sensor plane.

As the stage moves in steps of Δd from the reference plane, at each step, an image is captured in which barring a small portion of the object, other regions are defocused by different degrees. This is because a real aperture camera cannot bring all the points of a 3D object into focus at the same time. Thus, a stack of space-variantly defocused observations is obtained. The shape of the object is determined by searching for those frames in which the object points come in focus. In order to find the frame in which any point of the 3D object comes into focus, in traditional SFF [1], a focus measure profile is computed for each pixel across the image stack. The focus measure at a point (k, l) in an image I is computed using the

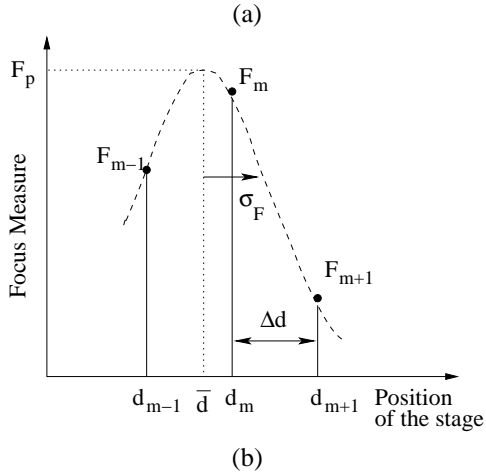
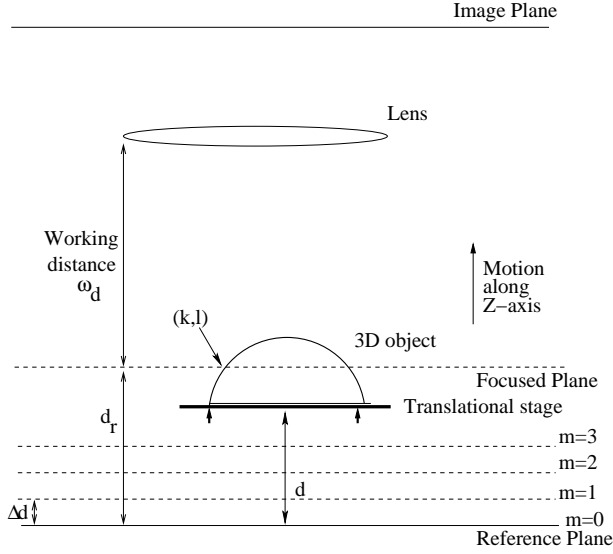


Fig. 1. (a) Schematic of traditional SFF. (b) Fitting the Gaussian function to the focus measure profile.

sum-modified Laplacian operator (SML) as

$$F(k, l) = \sum_{m=k-W}^{k+W} \sum_{n=l-W}^{l+W} O_L(m, n) \quad \text{for } O_L(m, n) \geq T_1 \quad (1)$$

where T_1 is a threshold, $2W + 1$ is the size of the window around the point (k, l) , and O_L is the modified Laplacian defined in the discrete domain as $O_L(m, n) = |2I(m, n) - I(m - \delta, n) - I(m + \delta, n)| + |2I(m, n) - I(m, n - \delta) - I(m, n + \delta)|$ where δ is a variable spacing between the image pixels for computing the derivatives. The focus measure profile for a pixel at (k, l) is obtained by plotting the value of $F(k, l)$ computed at (k, l) in every image of the stack starting from the reference frame. When the translating stage is at a height \bar{d} from the reference plane, the point (k, l) would reach the focused plane as shown in Fig. 1. Therefore, when $d = \bar{d}$ the value of the focus measure computed for the point (k, l) would be maximum as compared to other positions of the stage while moving through the stack. An estimate of the depth at (k, l) is arrived at by Gaussian interpolation of a few

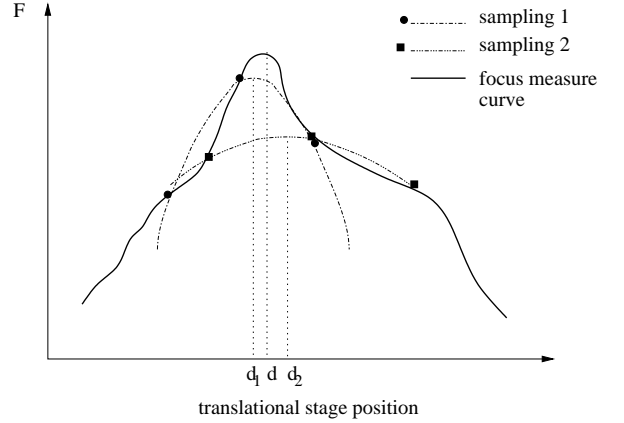


Fig. 2. Erroneous Gaussian interpolation in traditional SFF for different step-sizes [8]

values near the peak of the focus measure profile as shown in Fig. 1. The values of the focus measure for the point (k, l) corresponding to the heights of the translating stage from the reference plane of d_{m-1} , d_m and d_{m+1} are F_{m-1} , F_m and F_{m+1} . The Gaussian function with peak value F_p is fitted to these three focus measures. The mean of the fitted Gaussian function corresponding to pixel location (k, l) is denoted in Fig. 1 as \bar{d} . The values of \bar{d} calculated for all the points of the 3D object and denoted as \bar{d} yields the shape of the object.

A. Issues

As described above, the depth estimate of a point on a 3D object in the traditional SFF [1] method is arrived at using Gaussian interpolation of three values of focus measure near the peak of the focus measure profile. Since the Gaussian model is a good fit only in the peak region of the largest mode of the focus measure plot [1], the outcome of interpolation depends on whether the plot gets adequately sampled in that region. If the three focus measure values that are used for interpolation do not lie in the peak region of the actual focus measure plot, interpolation would result in an erroneous estimate of depth. The shape of the focus measure profile depends upon the local texture in the scene and the choice of the finite step size Δd is empirical which lead to a scenario as depicted in Fig. 2. The actual continuous focus measure profile of a point on an object is denoted by a solid line. The true value of the depth is d corresponding to the peak of the solid curve. Two different sampling scenarios are depicted for two different choices of Δd with dotted lines. For the first sampling of the continuous focus measure profile, shown by the dotted line joining points marked with \bullet , fitting a Gaussian function through the three strongest focus measure values gives a depth estimate as d_1 . In another sampling case shown by the dotted line joining the \blacksquare points, Gaussian interpolation yields the depth estimate as d_2 . Both d_1 and d_2 are erroneous estimates of the actual depth d because the actual focus measure curve has not been adequately sampled in the vicinity of its peak. This drawback of traditional SFF has been pointed out in [8].

In SFF, depth computation for a particular point of the 3D object is done independent of the neighbouring points. This can result in spurious spikes in the depth profile due to sudden variations in the shape of the focus measure plot. Real-world objects are locally smooth but this constraint is not used to guide depth computation. The shape of the focus measure profile is dependent on the local scene texture. If the region in the scene lacks sufficient texture, the focus measure plot is very smooth leading to errors in depth estimation by Gaussian interpolation. We believe that by utilizing information present in the real image data, i.e. the stack of observations captured in SFF, it would be possible to improve upon the depth estimates. Extending the work in [8], in this work we use information embedded in real images to recover a better depth map than in traditional SFF.

III. IMAGE FORMATION

Suppose the image plane consists of $M \times M$ sensor elements. Let the image intensity values be denoted by $\{y(i, j)\}$, $(i, j) = 0, 1, \dots, M - 1$. The space-variant blurring of an image of the 3D object in SFF can be expressed as

$$g(i, j) = \sum_k \sum_l x(k, l)h(i, j; k, l) \quad (2)$$

where $h(i, j; k, l)$ is a space-variant blurring function and $\{x(i, j)\}$ is the focused image. Observation noise when added to $\{g(i, j)\}$ yields the observed image $\{y(i, j)\}$ in the SFF stack.

A point on the 3D object at a distance $D' = w_d$ from the lens satisfies the lens law such that $\frac{1}{f} = \frac{1}{D'} + \frac{1}{v}$ and will be in focus on the sensor plane which is at a distance v from the lens plane. Here f denotes the focal length. Points that are not at distance D' from the lens plane will appear blurred. The point spread function (PSF) of a camera is defined as the response of the camera to a point light source. A point light source at distance D from the lens plane will be imaged on the sensor plane as a circular disk called the circle of confusion with radius $r_b = Rv\left(\frac{1}{f} - \frac{1}{v} - \frac{1}{D}\right)$ where R is the radius of the aperture of the lens. Due to diffraction and lens aberrations, the PSF is best described by a circularly symmetric 2D Gaussian function [10]

$$h(x, y) = \frac{1}{2\pi\sigma^2} \exp\left(-\frac{x^2 + y^2}{2\sigma^2}\right) \quad (3)$$

where $\sigma = \rho r_b$ and ρ is a camera constant. Several works [11], [12], [13] exist that validate the approximation of the true camera PSF by a 2D Gaussian. Since σ depends on D as

$$\sigma = \rho Rv \left(\frac{1}{f} - \frac{1}{v} - \frac{1}{D} \right) \quad (4)$$

the blur kernel $h(\cdot; \cdot)$ is space-varying and has the form

$$h(i, j; k, l) = \frac{1}{2\pi\sigma^2(k, l)} \exp\left(-\frac{(i-k)^2 + (j-l)^2}{2\sigma^2(k, l)}\right) \quad (5)$$

As the translating stage is moved vertically in steps of Δd , for the m^{th} frame we can express the blur parameter at (i, j)

as

$$\sigma_m(i, j) = \rho Rv \left(\frac{1}{w_d} - \frac{1}{w_d - m\Delta d + \bar{d}(i, j)} \right) \quad (6)$$

When the separation between the stage and the reference plane becomes \bar{d} , i.e. $m\Delta d = \bar{d}(i, j)$, the 3D point whose image pixel coordinates are (i, j) satisfies lens law, and will appear in perfect focus.

Suppose, the stack of observations available in SFF, contains N frames $\{y_m(i, j)\}$, $m = 1, 2, \dots, N$, each of size $M \times M$. These are blurred and noisy versions of a single focused image $\{x(i, j)\}$ of size $M \times M$. If \mathbf{y}_m is the lexicographically arranged vector containing pixels from the m^{th} observed image of size $M^2 \times 1$ and \mathbf{x} is the lexicographically arranged vector containing pixels from the original focused image of size $M^2 \times 1$, then they can be related as

$$\mathbf{y}_m = \mathbf{H}_m(\bar{\mathbf{d}})\mathbf{x} + \mathbf{n}_m, \quad m = 1, \dots, p \quad (7)$$

where $\mathbf{H}_m(\bar{\mathbf{d}})$ is a blur matrix of size $M^2 \times M^2$ that depends on $\bar{\mathbf{d}}$. Noise \mathbf{n}_m is zero mean Gaussian of size $M^2 \times 1$ with variance σ_η^2 .

When the 3D object is placed on the translational stage which is at the reference plane as shown in Fig. 1, the blur induced by a point on the object in the reference frame is governed by blur parameter σ_0 which is given by

$$\sigma_0 = \rho Rv \left(\frac{1}{w_d} - \frac{1}{D_0} \right) \quad (8)$$

where D_0 is the distance of the object point from the lens when the stage is at the reference position and w_d is the working distance of the camera i.e., $\frac{1}{w_d} = \frac{1}{f} - \frac{1}{v}$. The stage is moved vertically by a distance of $m \Delta d$ to capture the m^{th} LR frame. For the same point on the 3D object, the blurring induced in the m^{th} frame can be expressed by the blur parameter σ_m which is given by

$$\sigma_m = \rho Rv \left(\frac{1}{w_d} - \frac{1}{D_0 \pm m\Delta d} \right) \quad (9)$$

The change in magnification across the stack of LR observations is assumed to be negligible so that there are no errors due to registration. Eliminating the common term w_d from the above expressions for σ_m and σ_0 we get

$$\sigma_m = \sigma_0 + \rho Rv \left(\frac{1}{D_0} - \frac{1}{D_0 \pm m\Delta d} \right) \quad (10)$$

Using $\bar{\mathbf{d}}$ computed by the SFF method the blur parameter σ_0 at every point in the reference image can be computed. The blur parameter σ_m at any point in the m^{th} observation, $m = 1, 2, \dots, p$, can be determined with the knowledge of σ_0 at the same point in the reference frame using the relationship in Eq. 10. It is to be noted that the values of σ_m depend upon the depth map $\bar{\mathbf{d}}$ of the 3D object. Hence, the blurring matrix $\mathbf{H}_m(\bar{\mathbf{d}})$ in Eq. 7 can be constructed with the knowledge of σ_m .

In Eq. 10, it is important to note that the value of ρRv remains constant during the entire image capturing process.

IV. THE PROPOSED METHOD

The problem that we address here is the extraction of the shape profile $\bar{\mathbf{d}}$ of the 3D object, given p space-variantly blurred observations chosen from the stack in SFF, the focus measure profiles for all points on the object, and the focused image \mathbf{x} . The problem of estimation of the depth profile of the 3D object from the space-variantly blurred 2D images captured in SFF is typically ill-posed. Regularization in the form of a priori constraints on the solution can be imposed to estimate the depth map. Real-world 3D objects have depth profiles which are locally smooth. To incorporate spatial dependencies of the depth estimates on neighbouring points, we model $\bar{\mathbf{d}}$ as a Markov random field. Using Bayes' rule we can write

$$\log P(\bar{\mathbf{d}}|\mathbf{y}_1, \mathbf{y}_2, \dots, \mathbf{y}_p) = \log P(\mathbf{y}_1, \mathbf{y}_2, \dots, \mathbf{y}_p|\bar{\mathbf{d}}) + \log P(\bar{\mathbf{d}}) \quad (11)$$

where $\mathbf{y}_1, \mathbf{y}_2, \dots, \mathbf{y}_p$ are the p chosen observations from the stack.

MRFs can encode contextual constraints as well as provide a prior distribution with which to model the probability density function (pdf) of the depth map [14]. The Markovian property of the MRF states that the probability of a pixel being assigned a particular depth value depends only on the depth estimates of pixels in its neighbourhood. The Hammersley-Clifford theorem [15] provides the all-important equivalence between MRF and the Gibbs random field (GRF). If the shape profile $\bar{\mathbf{d}}$ is modeled as a Gauss-Markov random field (GMRF) then

$$P(\bar{\mathbf{d}}) = \frac{1}{Z} \exp \left[- \sum_{c \in C} V_c(\bar{\mathbf{d}}) \right] \quad (12)$$

where Z is the partition function, c is a clique, C is the set of all cliques and $V_c(\cdot)$ is the potential associated with clique c . For a first-order neighbourhood, we propose

$$\sum_{c \in C} V_c(\bar{\mathbf{d}}) = \sum_{i=1}^M \sum_{j=1}^M \frac{1}{F^2(i, j)} [(\bar{d}(i, j) - \bar{d}(i, j-1))^2 + (\bar{d}(i, j+1) - \bar{d}(i, j))^2 + (\bar{d}(i+1, j) - \bar{d}(i, j))^2 + (\bar{d}(i, j) - \bar{d}(i-1, j))^2] \quad (13)$$

Assuming the noise process \mathbf{n}'_m 's to be independent in Eq. 7, from Eqs. 11 and 13

$$\log P(\bar{\mathbf{d}}|\mathbf{y}_1, \mathbf{y}_2, \dots, \mathbf{y}_p) = - \sum_{m=1}^p \frac{\|\mathbf{y}_m - \mathbf{H}_m(\bar{\mathbf{d}})\mathbf{x}\|^2}{2\sigma_\eta^2} - \sum_{c \in C} V_c(\bar{\mathbf{d}}) \quad (14)$$

We derive an estimate of $\bar{\mathbf{d}}$ by minimizing the following

objective function

$$\hat{\bar{\mathbf{d}}} = \arg \min_{\bar{\mathbf{d}}} \left\{ \sum_{m=1}^p \frac{\|\mathbf{y}_m - \mathbf{H}_m(\bar{\mathbf{d}})\mathbf{x}\|^2}{2\sigma_\eta^2} + \lambda_1 \sum_{i=1}^M \sum_{j=1}^M \frac{1}{F^2(i, j)} [(\bar{d}(i, j) - \bar{d}(i, j-1))^2 + (\bar{d}(i, j+1) - \bar{d}(i, j))^2 + (\bar{d}(i+1, j) - \bar{d}(i, j))^2 + (\bar{d}(i, j) - \bar{d}(i-1, j))^2] \right\} \quad (15)$$

Note that we also incorporate the focus measure into the minimization procedure. Here $F(i, j)$ denotes the SML focus measure value at pixel location (i, j) . The SML focus measure operator is expected to yield a high value whenever the pixel at a particular location comes into focus in a certain frame in the stack of observations captured in SFF. The focus measure values are normalized such that the maximum value is unity. Being in the denominator, the SML values adaptively control the degree of smoothness for the estimation of the depth of a particular point on the 3D specimen. The focus measure profiles are obtained by applying the traditional SFF technique on the stack of observations. However, these values exist only for the positions of the translating stage through the entire stack. When the value of \bar{d} for a point lies in between two frame positions we use bilinear interpolation to compute its focus measure.

Assignment of depth values to pixel locations is a combinatorial optimization problem and we use iterated conditional modes (ICM), a fast but suboptimal technique [9]. The parameter λ_1 in Eq. 15 is tuned to obtain a good estimate of $\bar{\mathbf{d}}$.

In Eq. 15, we have assumed that the focused image \mathbf{x} of the 3D object is available. To an approximation and to avoid the additional burden of computing \mathbf{x} , one can estimate \mathbf{x} in the following manner. The formation of a pixel $y(i, j)$ in an observed image can be expressed as

$$y(i, j) = \sum_k \sum_l x(k, l)h(i, j; k, l) + n(i, j) \quad (16)$$

During the imaging of a particular frame, if the corresponding point (i, j) on the 3D object was on the focused plane, it would satisfy the lens law and hence would be perfectly focused on the image plane. If the point (i, j) lies in a smooth region in the 3D object, the blur induced in it due to the space-variant defocusing mechanism by neighbouring pixels would also be negligible. This is because the neighbouring points would also be very close to the focused plane. Assuming that the noise during image capture is low, the intensity value of $y(i, j)$ from that frame in the stack can be chosen as an estimate of the intensity of the focused image \mathbf{x} at pixel (i, j) . Since the whole stack of frames is available with us, for every point on the 3D object, we can choose the frame in which each point comes into focus and pick the corresponding pixel intensity for \mathbf{x} from that frame. This allows us to construct a reasonable approximation of the focused image.

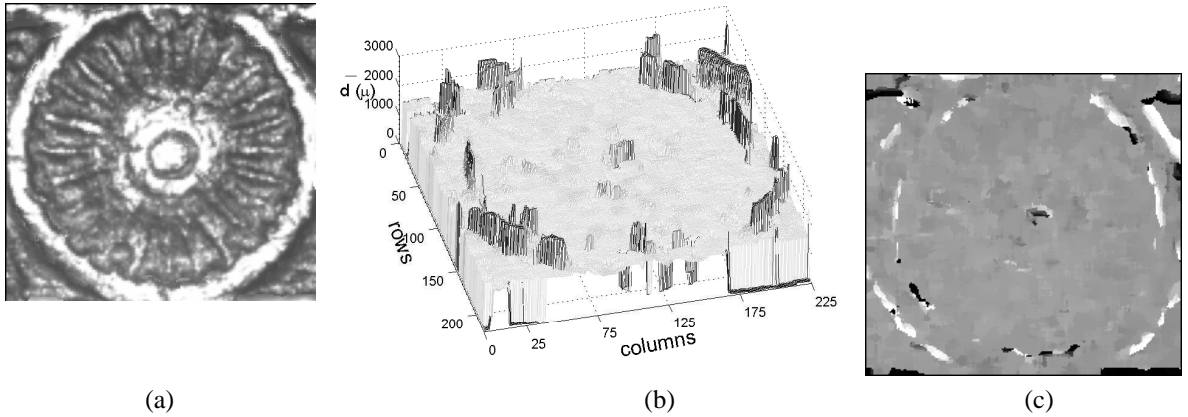


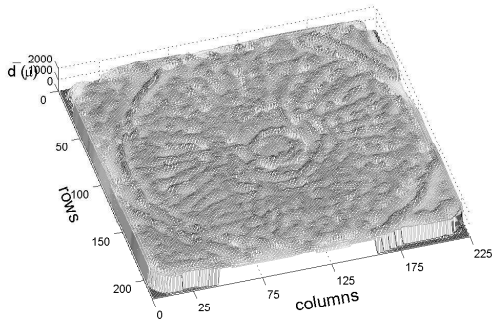
Fig. 3. (a) Focused image of a portion of a coin. (b) Estimated depth map obtained using the traditional SFF algorithm. (c) Grayscale image of the corresponding depth map.

V. EXPERIMENTAL RESULTS

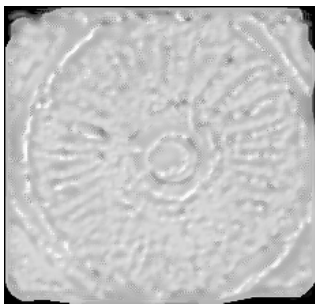
An LV-150 Nikon industrial microscope was used for imaging. The lens objective was 2.5x, the working distance $w_d = 8.8$ mm, focal length $f = 80$ mm and the depth of field = $48.9 \mu\text{m}$. The PSF of the camera was assumed to be Gaussian, which is a reasonable approximation as discussed in section 3.

We present experimental results using a coin as the 3D

specimen. A stack of 150 frames, of size 220×230 pixels, was captured by moving the translating stage of the microscope in



(a)

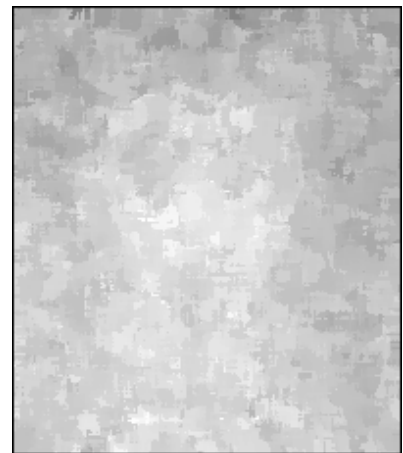


(b)

Fig. 4. Optimized by ICM (a) Estimated shape obtained using the proposed algorithm. (b) Grayscale image of the corresponding shape profile.

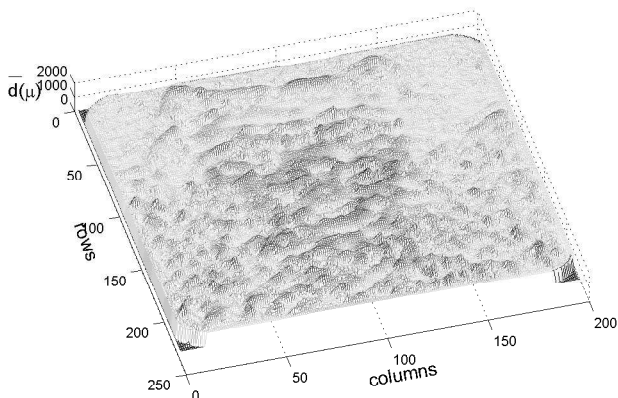


(a)

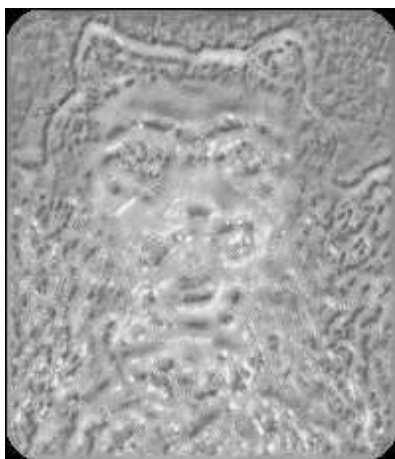


(b)

Fig. 5. (a) Focused image of another portion of a coin. (b) Grayscale image of the corresponding estimated depth map obtained using the traditional SFF algorithm.



(a)



(b)

Fig. 6. Optimized by ICM (a) Estimated shape obtained using the proposed algorithm. (b) Grayscale image of the corresponding shape profile.

fixed steps of $\Delta d = 0.025$ mm. The focused image of the specimen is shown in Fig. 3 (a). The traditional SFF method is used to obtain the depth map which is given in Fig. 3 (b). The grayscale image of this depth map is shown in Fig. 3 (c). It can be observed that the spokes of the wheel are not visible. The depth map obtained from the traditional SFF method is smoothed by median filtering and is used as the initial estimate of the shape profile. The proposed algorithm is next used to estimate the depth map. The focus measure profiles for every pixel earlier obtained in computing the depth map were used in the proposed method. The cost function in equation (15) is minimized using the ICM algorithm and the estimate of the shape is shown in Fig. 4 (a). The algorithm converges in 5 - 6 iterations. In all our experiments, the values of $\lambda_1 = 1 \times 10^8$ and $\sigma_\eta^2 = 5$ in the proposed cost function. The grayscale image of the shape profile is shown in Fig. 4 (b). The spokes of the wheel and other details are clearly visible now.

For the next example, we imaged another portion of the same coin, wherein the head of a lion is depicted. By moving the translating stage of the microscope in fixed steps of 0.025 mm, a stack of 100 frames is captured. Each of the images

captured is of size 228×198 pixels. The focused image obtained is shown in Fig. 5 (a). The stack of observations are used to estimate the depth map using the traditional SFF algorithm. The grayscale image corresponding to the estimated depth profile is shown in Fig. 5 (b). The features of the head of the lion have not emerged well here.

The proposed method is then used to obtain an estimate of the shape of the 3D object. Choosing frame numbers 15, 20, 65 and 70, the depth map is estimated by minimizing the proposed cost function and is shown in Fig. 6 (a). The grayscale image corresponding to this depth map is shown in Fig. 6 (b). Comparing Fig. 5 (b) and Fig. 6 (b), we can easily observe that the proposed algorithm has been successful in estimating the variations in depth over the engraving on the coin. Various features like the ears, eyes and the mouth region can be seen clearly.

VI. CONCLUSIONS

We proposed a method for improving the depth map estimated in traditional SFF. Using a few of the space-variantly blurred images from the captured stack, and the focus measure profiles for all the pixels, the shape of the 3D object was reconstructed. A degradation model was used to describe the image formation process in SFF. Incorporating spatial dependencies of shape estimates by modeling the shape as an MRF, considerable improvement in the quality of reconstruction of the structure of the object was obtained.

REFERENCES

- [1] S.K. Nayar and Y. Nakagawa, "Shape from focus," *IEEE Trans. Pattern Anal. Mach. Intell.*, vol. 16, no. 8, pp. 824-831, 1994.
- [2] M. Subbarao and T.S. Choi, "Accurate recovery of three-dimensional shape from image focus," *IEEE Trans. Pattern Anal. Mach. Intell.*, vol. 17, no. 3, pp. 266-274, 1995.
- [3] J. Yun and T.S. Choi, "Accurate 3-D recovery using curved window focus measure," *Proc. Int. Conf. Image Processing*, pp. 910-914, 1999.
- [4] M. Asif and T.S. Choi, "Shape from focus using multilayer feedforward neural networks," *IEEE Trans. Image Process.*, vol. 10, no. 11, pp. 1670-1675, 2001.
- [5] M.B. Ahmad and T.S. Choi, "A heuristic approach for finding best focused shape," *IEEE Trans. on Circuits and Systems for Video Technology*, vol. 15, no. 4, pp. 566-574, 2005.
- [6] M.B. Ahmad and T.S. Choi, "Shape from focus using optimization technique," *Proc. Int. Conf. Acoustics, Speech and Signal Processing*, pp. 493-496, 2006.
- [7] R.R. Sahay and A.N. Rajagopalan, "High resolution image reconstruction in shape from focus," *Proc. Int. Conf. Image Processing*, pp. 69-72, 2007.
- [8] K.S. Pradeep and A.N. Rajagopalan, "Improving shape from focus using defocus cue," *IEEE Trans. Image Process.*, vol. 16, no. 7, pp. 1920-1925, 2007.
- [9] J. Besag, "On the statistical analysis of dirty pictures," *J. Royal Statistical Soc., Series B*, vol. 48, pp. 259-302, 1986.
- [10] A.P. Pentland, "A new sense for depth of field," vol. 9, no. 4, pp. 523-531, 1987.
- [11] M. Born and E. Wolf, *Principles of optics*, Pergamon, 1965, London.
- [12] M. Subbarao, "Parallel depth recovery by changing camera parameters," *Proc. Int. Conf. Computer Vision*, pp. 149-155, 1988.
- [13] S. Chaudhuri and A.N. Rajagopalan, *Depth from defocus: A real aperture imaging approach*, Springer-Verlag, 1999, New York.
- [14] S.Z. Li, *Markov random field modeling in computer vision*, Springer-Verlag, 1995, Tokyo.
- [15] J. Besag, "Spatial interaction and the statistical analysis of lattice system," *J. Royal Statistical Soc., Series B*, vol. 36, pp. 192-236, 1974.